Supporting Information (SI1)

Copper Oxide nanomaterial fate in plant tissue: Nanoscale impacts on reproductive tissues

Marta Marmiroli,[1,*] Luca Pagano,[1,*] Riccardo Rossi,[1] Roberto De La Torre-Roche,[2] Giovanni Orazio Lepore,[3] Roberta Ruotolo,[1] Gianluca Gariani,[4] Valentina Bonanni,[4] Simone Pollastri,[4] Alessandro Puri,[5] Alessandra Gianoncelli,[4] Giuliana Aquilanti,[4] Francesco d'Acapito,[5] Jason C. White,[2,§] Nelson Marmiroli[1,6,§,#]

[1] Department of Chemistry, Life Sciences and Environmental Sustainability, University of Parma, Parco Area delle Scienze 11/A, 43124 Parma, Italy.

[2] The Connecticut Agricultural Experiment Station, 123 Huntington Street, 06504 New Haven, CT, USA.

[3] Dept. Scienze della Terra, Univeristy of Firenze, Via La Pira 4, 50121 Firenze, Italy.

[4] Elettra, Sincrotrone Trieste, Strada Statale 14 - km 163,5 in AREA Science Park, 34149 Trieste, Italy.

[5] CNR-IOM-OGG c/o ESRF - The European Synchrotron, 71 Avenue des Martyrs CS 40220, F38043 Grenoble Cédex 9, France.

[6] Consorzio Interuniversitario Nazionale per le Scienze Ambientali (CINSA), University of Parma, 43124 Parma, Italy.

* co-first authorship.

§ co-last authorship.

corresponding author, nelson.marmiroli@unipr.it.

Table of Contents

Supporting information 1 (SI1) ordered by citation in the main text:

Table S1: Biomass of roots and shoots.

Table S2: Flower biomass.

Table S3: Copper concentration measured in soil, roots, shoots and flowers by AAS.

Table S4: Copper concentration measured in flowers by ICP-MS.

Table S5: Genes information and primer sequences utilized in Real time PCR assay.

Table S6: EXAFS multiparameter fit details for studied samples and reference compounds.

Supporting information (in excel format):

Supplementary Information 2 (SI2): GO analysis of up- and down-regulated genes exposed to CuO NPs, CuO bulk and $CuSO_4$ in roots.

Supplementary Information 3 (SI3): GO analysis of up- and down-regulated genes exposed to CuO NPs, CuO bulk and $CuSO_4$ in leaves.

Supplementary Information 4 (SI4): GO analysis of up- and down-regulated genes exposed to CuO NPs, CuO bulk and $CuSO_4$ in pollen.

Supplementary Information 5 (SI5): *A. thaliana* ortholog genes analysis of relevant chloroplast and mitochondrial targets isolated from *C. pepo* exposed to CuO NPs, CuO bulk and $CuSO_4$ in roots, leaves and pollen.

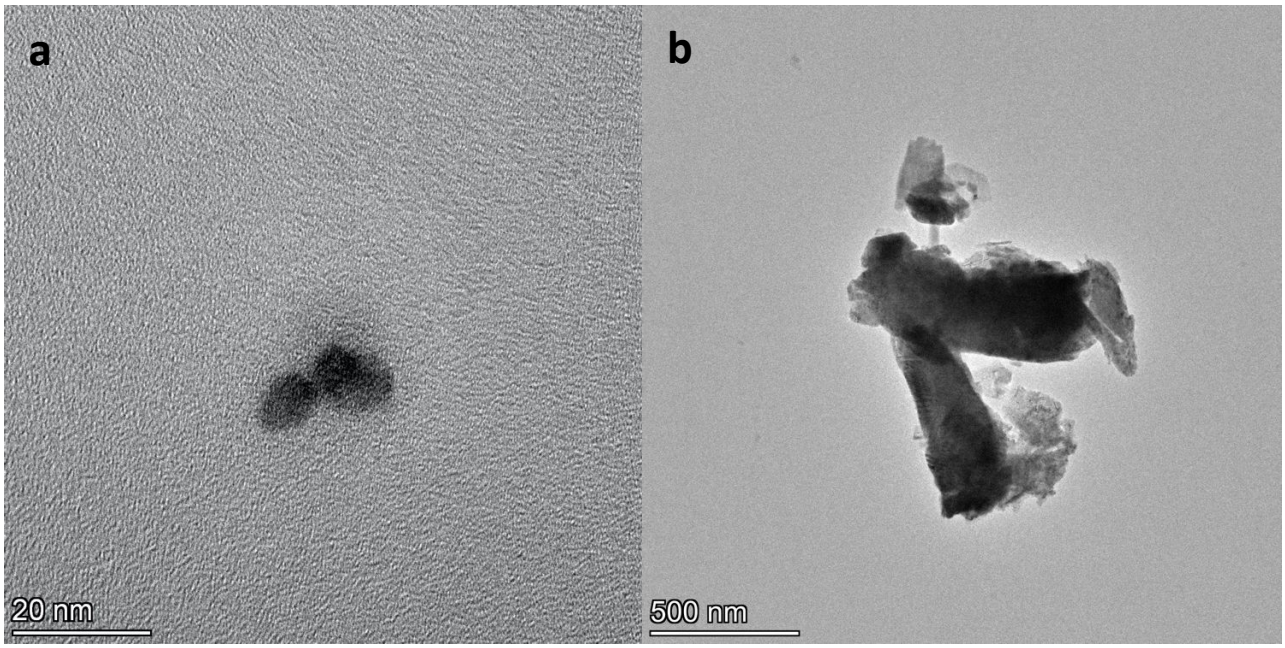

Figure S1. CuO nanoparticles (a) and their aggregates (b) observed by TEM, Talos F200S G2, FEG (Thermo Fisher Scientific, Waltham, MA, USA). The results align with the average particle size (*dh*) in ddH_2O of 533.9 nm, measured by Zetasizer Nano Series ZS90 (Malvern Instruments, Malvern, UK).

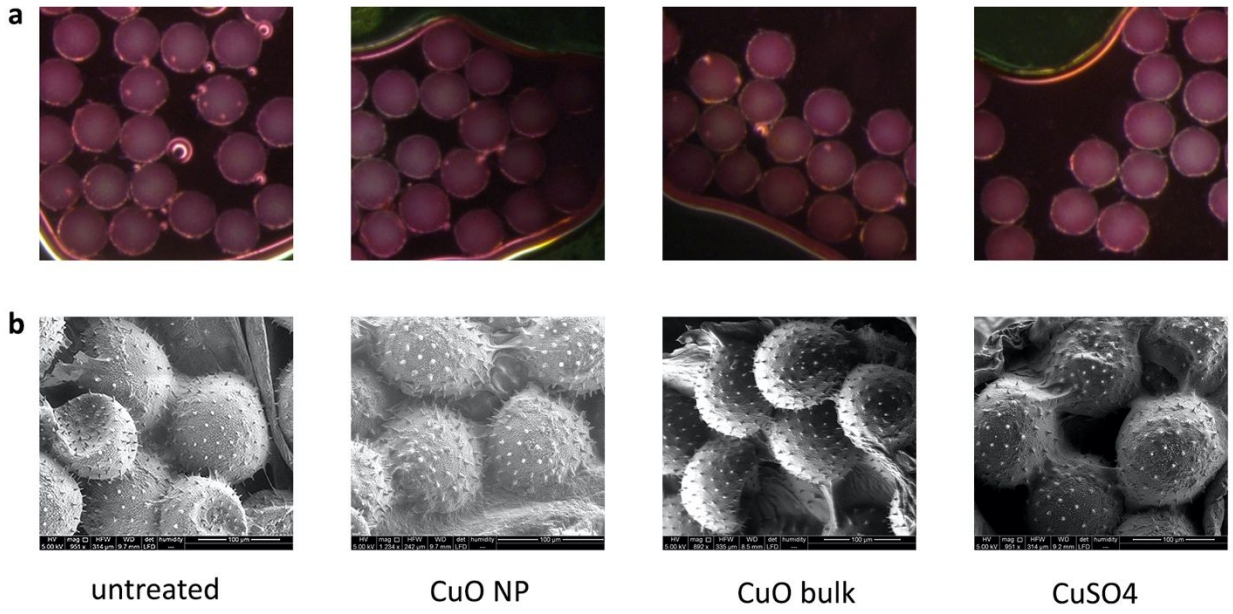

Figure S2. (a) Pollen viability measured by Alexander's staining protocol and (b) ESEM micrographs of fresh pollen grains. Non-aborted pollen grains were observed in all the treatments reported (in magenta red). No significant differences were observed in shape and viability between treatments.

Table S1. Biomass of plant roots and shoots (fresh weight, expressed in g) treated with 100 mg Kg^{-1} of CuO NPs, CuO bulk, and 320 mg Kg^{-1} $CuSO_4$ (representing a total concentration of Cu about 80 mg kg^{-1} for all the treatments) with relative standard deviation and Tukey's (HSD) pairwise multiple comparisons ($p < 0.05$).

Roots	**sample**	**biomass**	**stdev**	**%**	**HSD**
	untreated	1.808	0.237	100	A
	CuO NPs	2.344	0.744	129.646	A
	CuO Bulk	2.755	0.637	152.378	A
	$CuSO_4$	1.960	0.314	108.407	A

Shoots	**sample**	**biomass**	**stdev**	**%**	**HSD**
	untreated	27.43	3.480	100	A
	CuO NPs	32.68	1.940	119.116	A
	CuO Bulk	29.92	3.200	109.084	A
	$CuSO_4$	31.32	5.440	114.159	A

Table S2. Flower biomass (fresh weight, expressed in g) from plants treated with 100 mg Kg^{-1} of CuO NPs, CuO bulk representing a total concentration of Cu about 80 mg Kg^{-1} for all the treatments) with relative standard deviation and Tukey's (HSD) pairwise multiple comparisons ($p < 0.05$). Data refer to ICP-MS analyses.

Flowers	sample	biomass	stdev	%	HSD
	untreated	1.327	0.370	100	A
	CuO NPs	1.233	0.450	92.879	A
	CuO Bulk	1.572	0.220	118.438	A

Table S3. Copper availability in soil and copper concentration measured in roots, shoots and flowers (expressed in mg Kg^{-1}) by Atomic Absorption Spectrometry (AAS) with relative standard deviation and Tukey's (HSD) pairwise multiple comparisons ($p < 0.05$). (*) relative percentage of available Cu, as compared to the treatment concentration (about 80 mg Kg^{-1}) calculated after dissolution in soil for 14d and normalized on the untreated soil Cu concentration (14.18 mg Kg^{-1}).

Soil	sample	Cu conc	stdev	free Cu*
	CuO NPs	0.305	0.032	0.34%
	CuO Bulk	0.050	0.002	0.05%
	CuSO4	0.488	0.011	0.56%

Roots	sample	Cu conc	stdev	HSD
	untreated	40.593	11.250	A
	CuO NPs	43.181	5.078	A
	CuO Bulk	69.384	15.419	A
	CuSO4	110.500	34.672	B

Shoots	sample	Cu conc	stdev	HSD
	untreated	7.466	2.495	A
	CuO NPs	9.157	1.288	A
	CuO Bulk	14.353	4.675	A
	CuSO4	14.750	1.167	A

Flowers	sample	Cu conc	stdev	HSD
	untreated	15.968	1.343	A
	CuO NPs	17.158	0.839	AB
	CuO Bulk	18.435	3.291	AB
	CuSO4	20.082	2.281	B

Table S4. Copper concentration (expressed in mg kg^{-1}) measured in flowers by ICP-MS (expressed in mg kg^{-1}) as a function of treatment with CuO NP or bulk (100 mg L^{-1}), with relative standard deviation and Tukey's (HSD) pairwise multiple comparisons ($p < 0.05$).

Flowers	sample	Cu conc	stdev	HSD
	untreated	7.93	0.70	A
	CuO NPs	13.80	2.00	B
	CuO Bulk	11.30	1.50	B

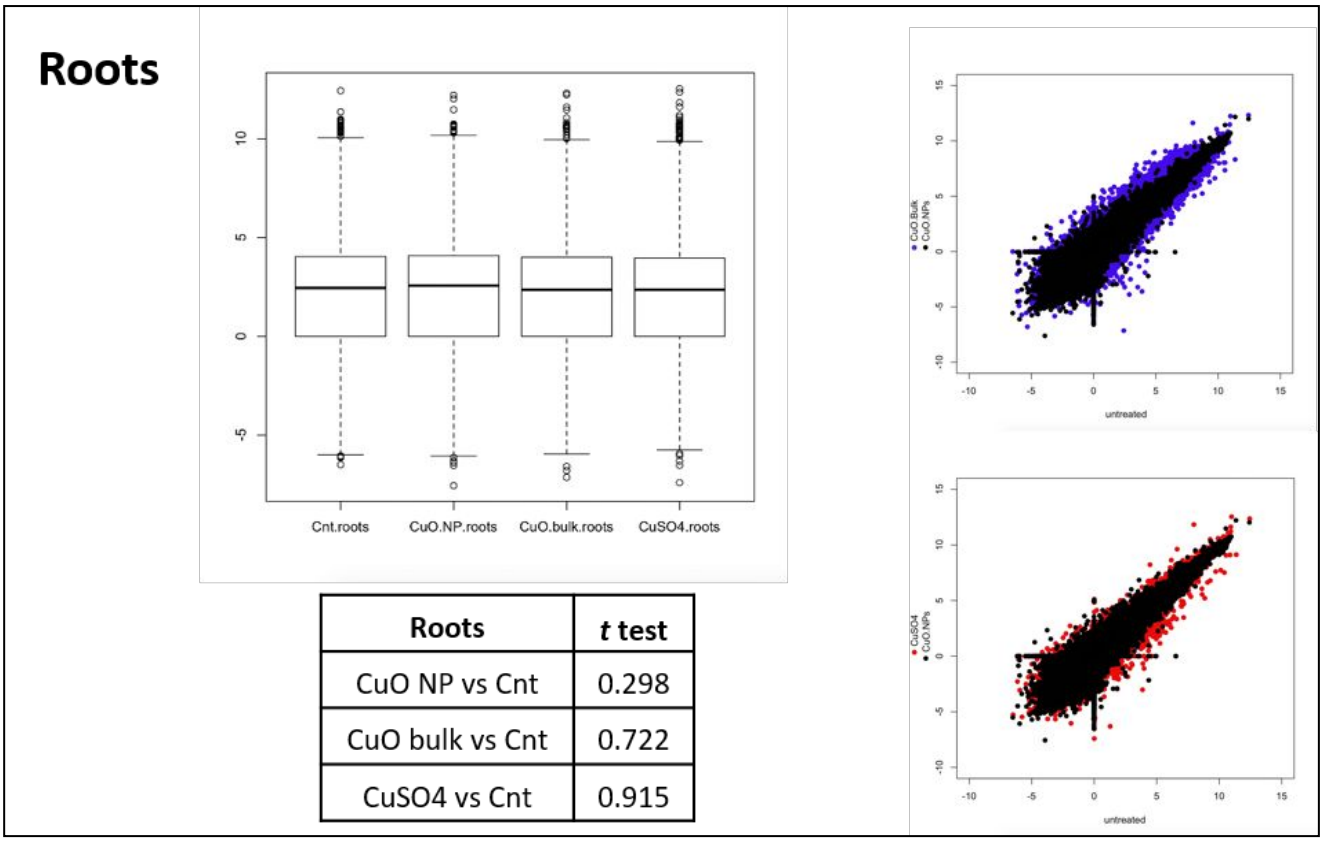

Roots	*t* test
CuO NP vs Cnt	0.298
CuO bulk vs Cnt	0.722
CuSO4 vs Cnt	0.915

Figure S3. Statistics of the RNAseq datasets from roots exposed to 100 mg Kg^{-1} of CuO NPs, CuO bulk, and 320 mg Kg^{-1} $CuSO_4$ (representing a total concentration of Cu about 80 mg Kg^{-1} for all the treatments). Box and wiskers plot related to data distribution and *t* test (control [cnt] vs sample) are reported in order to verify the homogenity of variance (on the right). Scatter plots show the data dispersion between CuO NPs (black) and CuO bulk (blue) or $CuSO_4$ (red). All data were normalized on the untreated control (cnt).

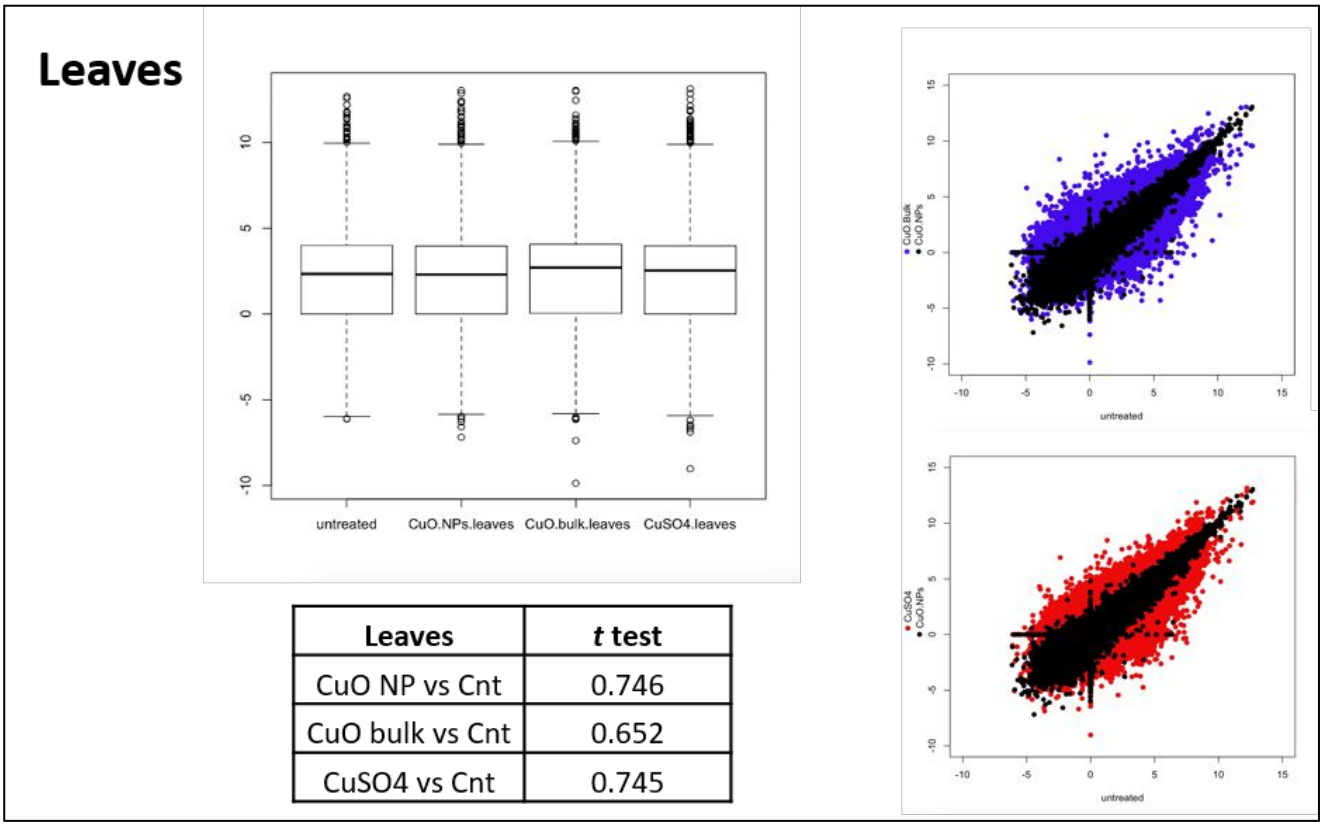

Leaves	*t* test
CuO NP vs Cnt	0.746
CuO bulk vs Cnt	0.652
CuSO4 vs Cnt	0.745

Figure S4. Statistics of the RNAseq datasets from leaves, exposed to 100 mg Kg^{-1} of CuO NPs, CuO bulk, and 320 mg Kg^{-1} $CuSO_4$ (representing a total concentration of Cu about 80 mg Kg^{-1} for all the treatments). Box and wiskers plot related to data distribution and *t* test (control [cnt] vs sample) are reported in order to verify the homogenity of variance (on the right). Scatter plots show the data dispersion between CuO NPs (black) and CuO bulk (blue) or $CuSO_4$ (red). All data were normalized on the untreated control (cnt).

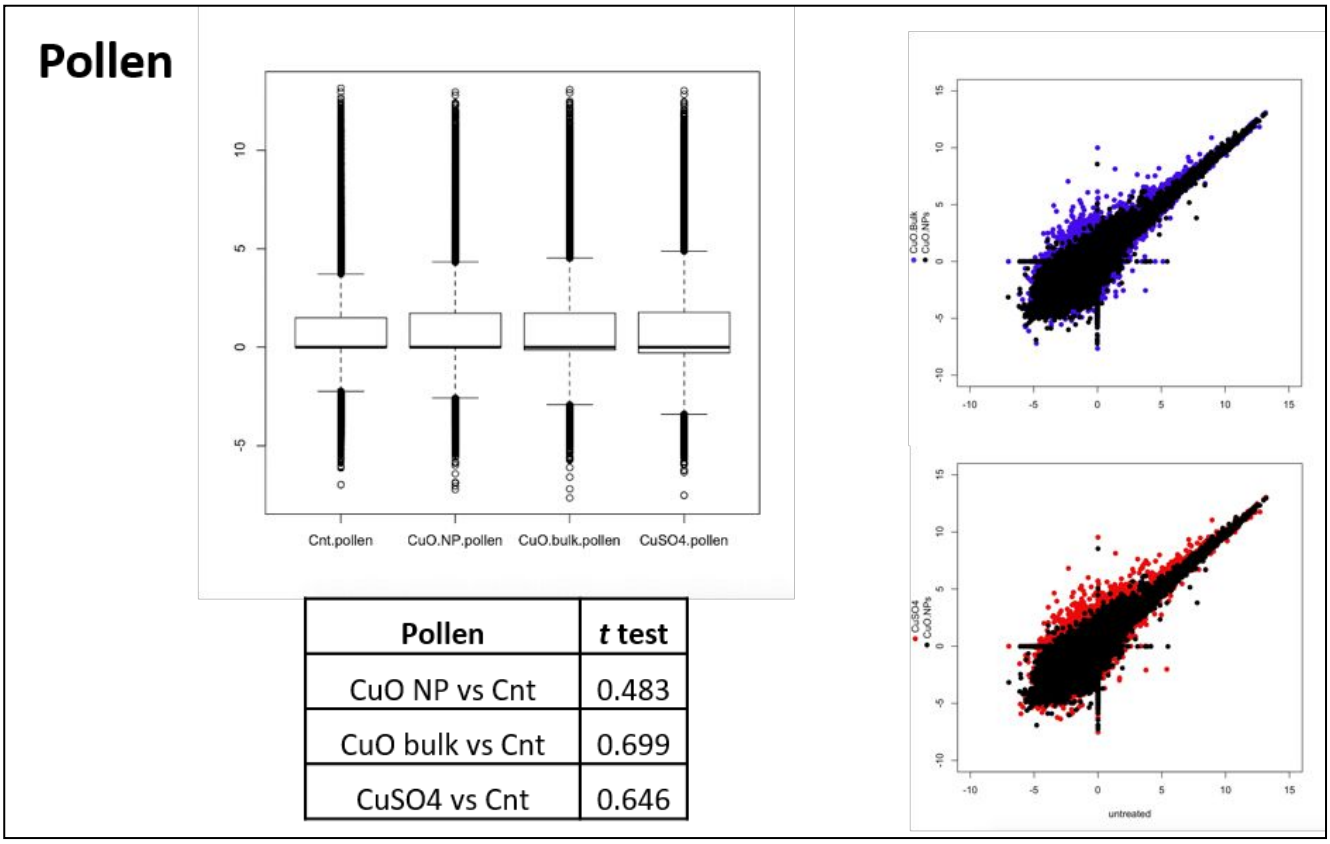

Pollen	*t* test
CuO NP vs Cnt	0.483
CuO bulk vs Cnt	0.699
CuSO4 vs Cnt	0.646

Figure S5. Statistics of the RNAseq datasets from pollen, exposed to 100 mg Kg^{-1} of CuO NPs, CuO bulk, and 320 mg Kg^{-1} $CuSO_4$ (representing a total concentration of Cu about 80 mg Kg^{-1} for all the treatments). Box and wiskers plot related to data distribution and *t* test (control [cnt] vs sample) are reported in order to verify the homogenity of variance (on the right). Scatter plots show the data dispersion between CuO NPs (black) and CuO bulk (blue) or $CuSO_4$ (red). All data were normalized on the untreated control (cnt).

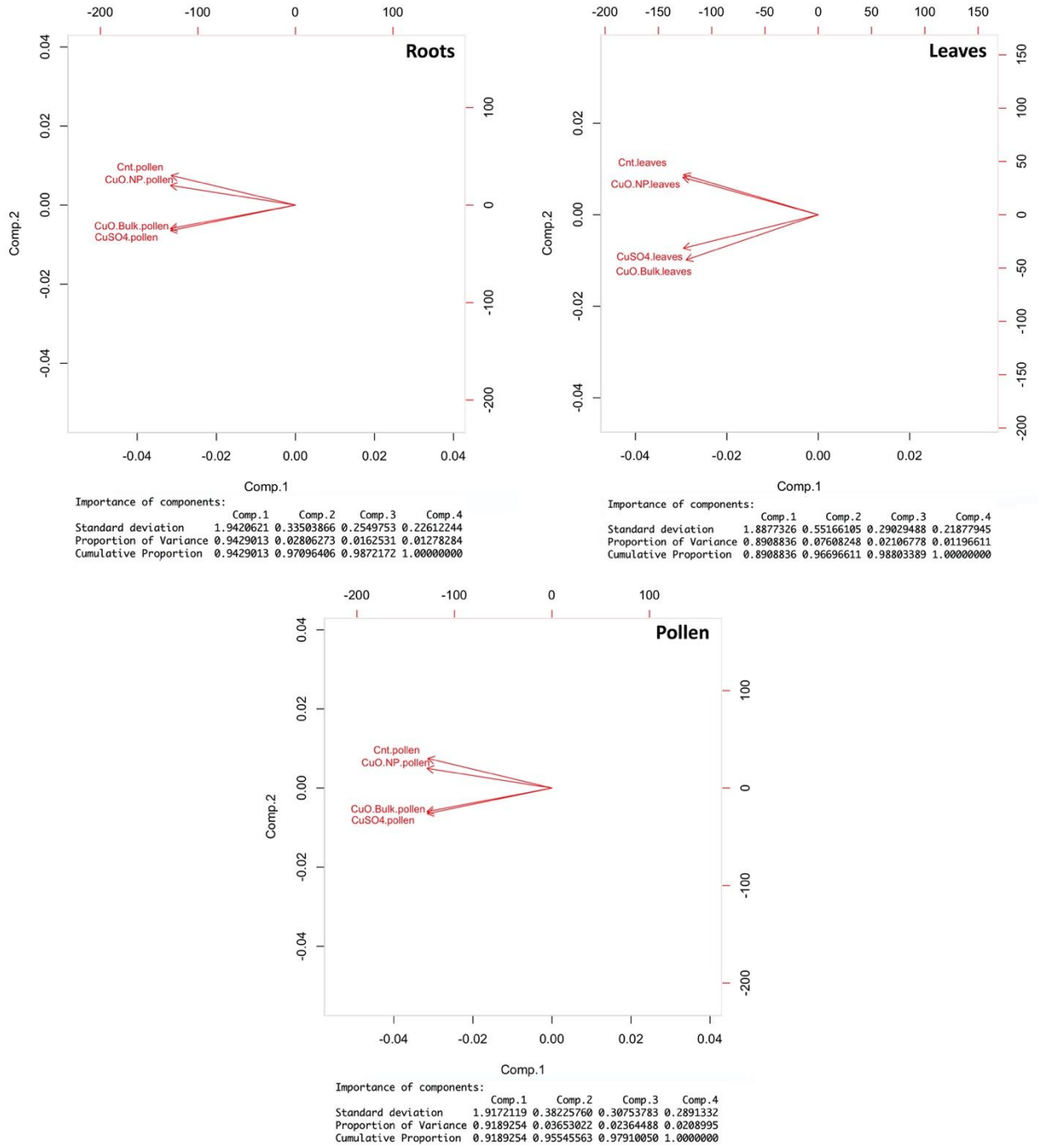

Figure S6. Principal component analysis (PCA) of the roots, leaf and pollen transcriptomic profiles. Data showed in all cases how CuO bulk and $CuSO_4$ responses were more to each other than to CuO NPs, suggesting a similar pathway of response.

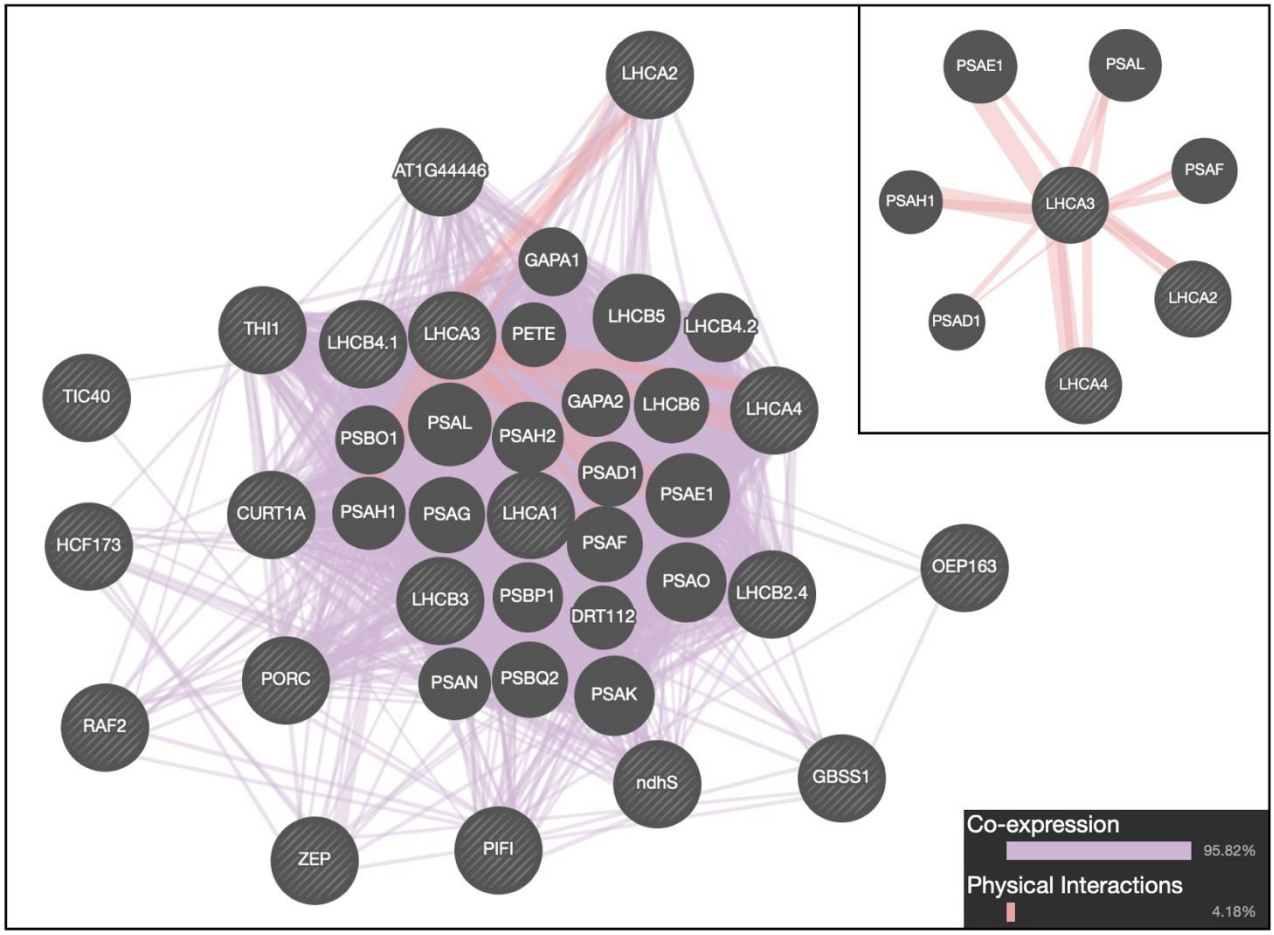

Figure S7. Gene network of chloroplast constructed with targets modulated in leaves and responsive to CuO NPs with their co-expression (purple) and physical interactions (pink), modelled on *Arabidopsis thaliana* genome. Ortholog gene identification were performed by the Cucurbitgenomics database (http://cucurbitgenomics.org/), while network generation have been performed using the GeneMANIA data service (http://www.genemania.org/). Query gene are indicated by stripes.

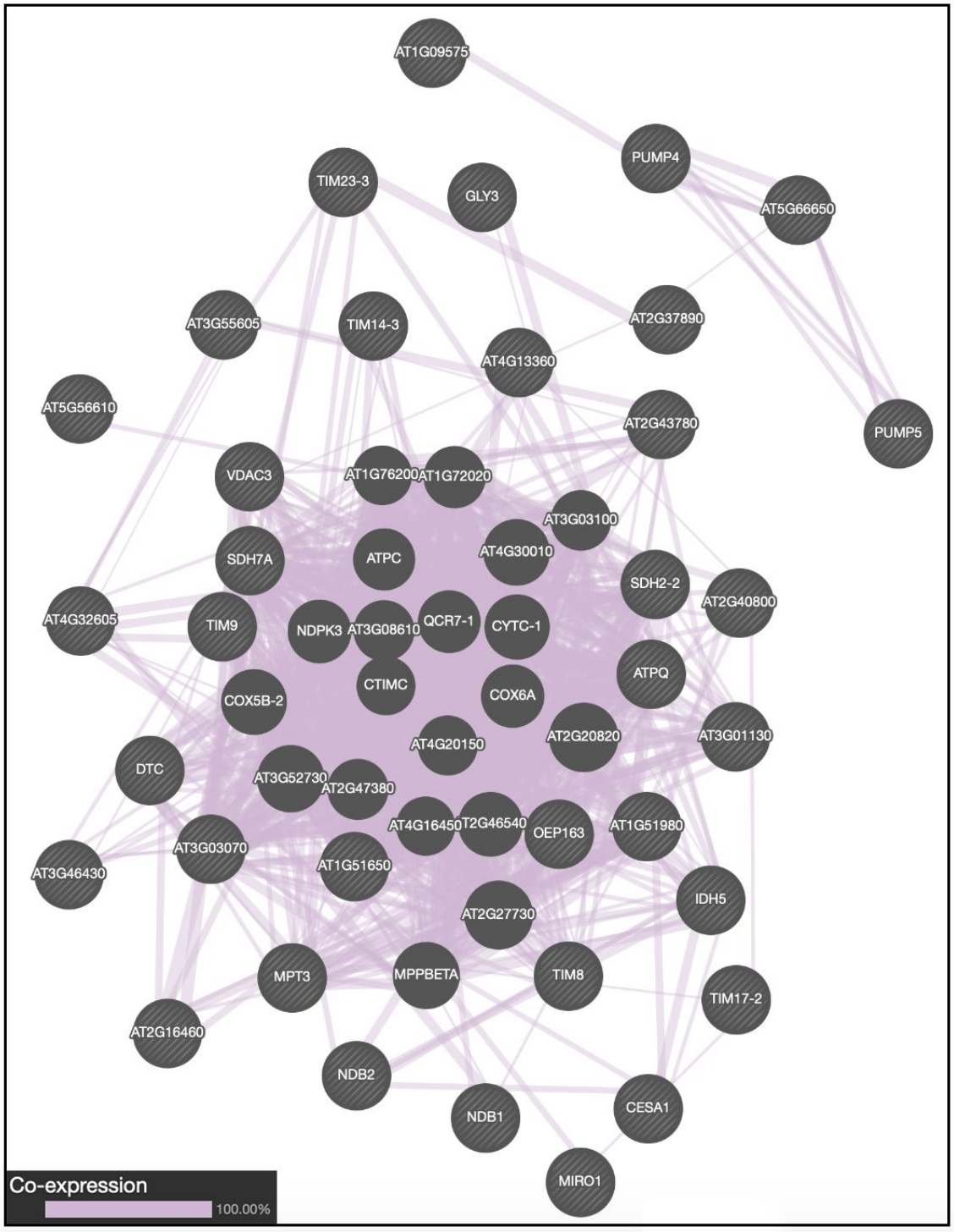

Figure S8. Gene network of mitochondria constructed with targets modulated in roots and responsive to CuO NPs with their co-expression (purple), modelled on *Arabidopsis thaliana*. Ortholog gene identification were performed by the Cucurbitgenomics database (http://cucurbitgenomics.org/), while network generation have been performed using the GeneMANIA data service (http://www.genemania.org/). Query gene are indicated by stripes.

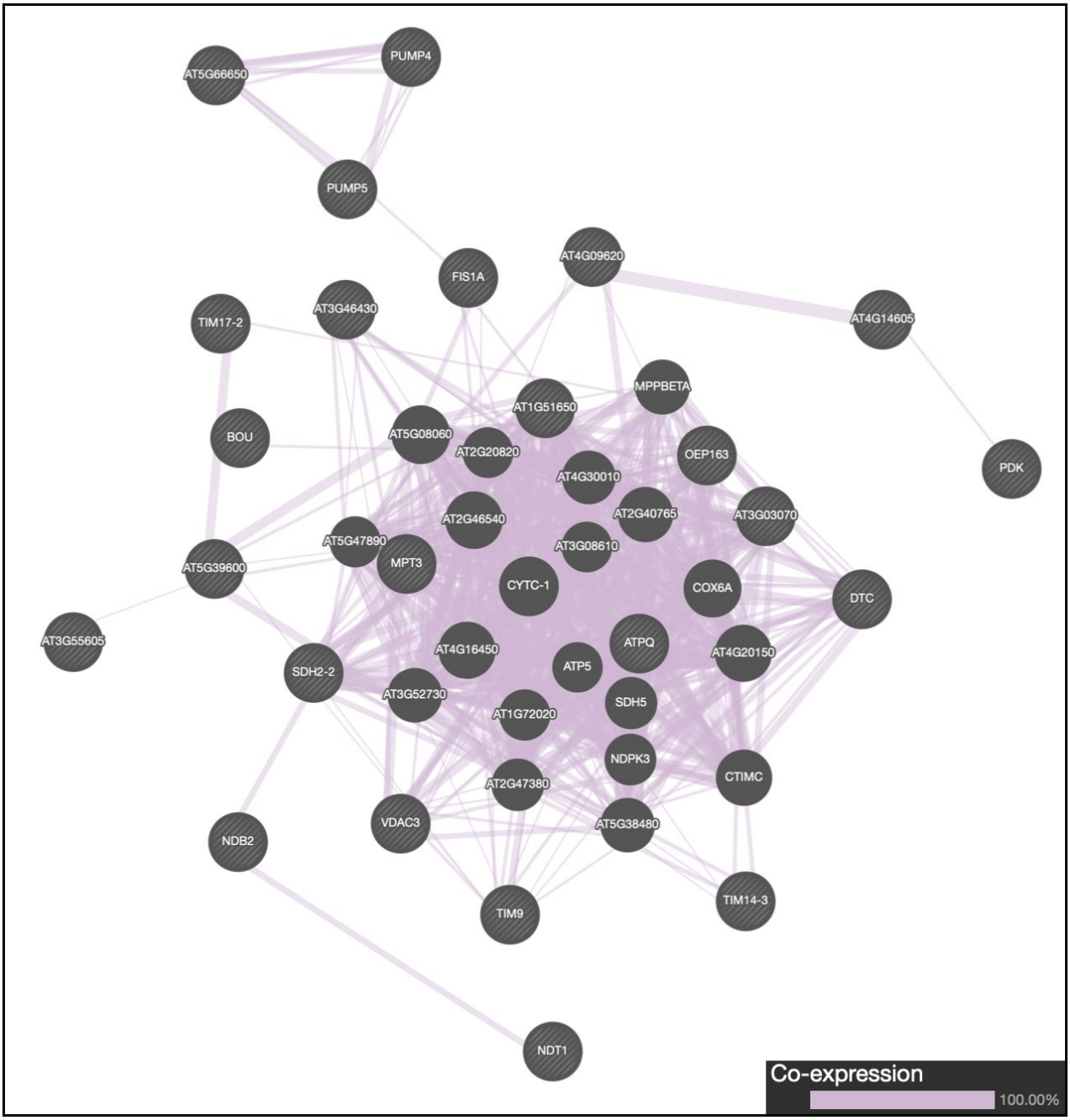

Figure S9. Gene network of mitochondria constructed with targets modulated in leaves and responsive to CuO NPs with their co-expression (purple), modelled on *Arabidopsis thaliana*. Ortholog gene identification were performed by the Cucurbitgenomics database (http://cucurbitgenomics.org/), while network generation have been performed using the GeneMANIA data service (http://www.genemania.org/). Query gene are indicated by stripes.

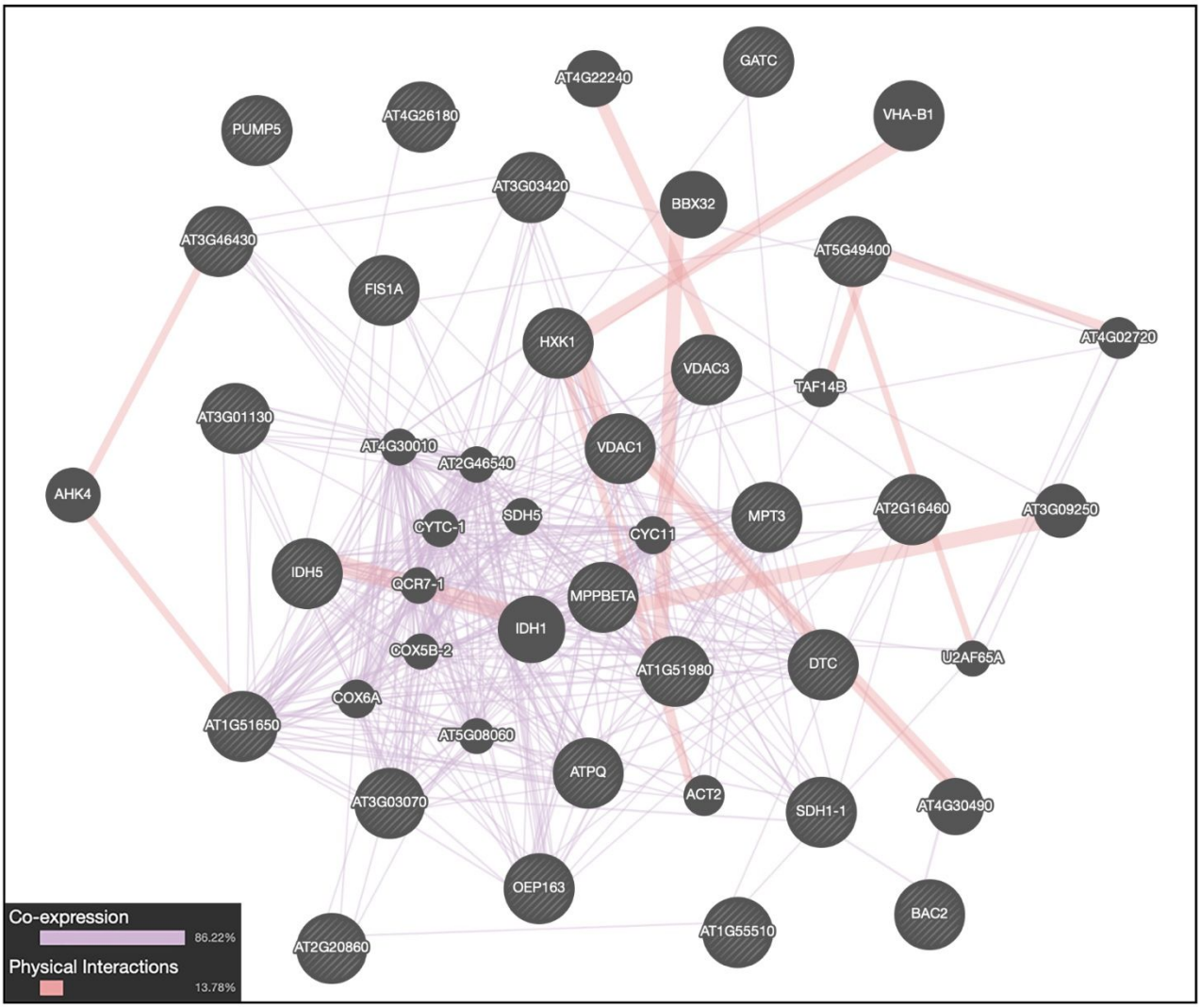

Figure S10. Gene network of mitochondria constructed with targets modulated in pollen and responsive to CuO NPs with Ortholog gene identification were performed by the Cucurbitgenomics database (http://cucurbitgenomics.org/), while network generation have been performed using the GeneMANIA data service (http://www.genemania.org/). Query gene are indicated by stripes.

Real Time quantitative PCR on genes involved in gametogenesis

Mature pollen was gently scraped from *C. pepo* anthers, transferred to a 1.5 ml tube, and frozen in liquid nitrogen. After extraction by Sigma-Aldrich Spectrum Plant Total RNA Kit (Sigma-Aldrich, St. Louis, MO), total RNA was quantified by NanoDrop (Thermo Fisher Scientific, Walthan, MA). One µg of total RNA for each sample was retrotranscribed using Qiagen Reverse transcription kit (Hilden, GER). cDNAs were quantified by Real Time PCR using a SYBR green Mastermix (Applied Biosystems, Foster City, CA), on ABI PRISM 7500 Sequence Detection System (Applied Biosystems), using primers for genes specifically expressed in mature pollen and during gametogenesis.[1] Primers sequences of the potential meiosis gene targets identified in the yeast *Saccharomyces cerevisiae* are included in Table S5. *C. pepo* ortholog gene identification was performed using the Cucurbitgenomics database (http://cucurbitgenomics.org/). Each reaction was conducted in triplicate. Signals were normalized on *ACT1* (*Cp4.1LG05g10740*) transcript levels. Relative transcript abundances were derived using the $2^{-\Delta\Delta Ct}$ method, with Student's *t* test ($p < 0.05$). Analysis did not show any genes in common with RNAseq analyses (Figure S11), though it showed some other potential sensitive candidates that were modulated by CuO NPs: three out of eight genes considered were differentially modulated between CuO NPs and bulk treatments: myb35 (*Cp4.1LG03g07890*), which encodes for a transcriptional activator required for anthers development and early tapetal function during pollen maturation; prd1 (*Cp4.1LG12g04800*), whose gene product is involved in meiotic recombination and in meiotic double strand break repair; mnd (*Cp4.1LG18g03910*), which encodes for a protein involved in DNA binding during meiotic process, stimulating the recombinase activity of Rad51 protein. This regulatory response can be considered specific for CuO NPs treatment, suggesting how bioavailable Cu release from nanoscale and bulk forms may have a differential impact during gametes formation.

Table S5. Genes' information and primer sequences utilized in Real time PCR, on potential targets involved in *C. pepo* gametogenesis, with particular regard to meiotic process.

name	***C. pepo* locus ID**	***C. pepo* gene ID**	**function**	**primer name**	**sequence**
act1	-	Cp4.1LG05g10740	Structural component cytoskeleton	act for	ACCCTCCAATCCAGACACTG
				act rev	TGACAGGATGAGCAAGGAAA
myb35	LOC111789794	Cp4.1LG03g07890	MYB class transcriptional factor	myb35 for	TGGACTGCAGAGGAAGATGC
				myb35 rev	CCCTGCTTTCTTGGGAACCA
serk2	LOC111797063	Cp4.1LG06g09610	Serine/threonine-kinase involved in brassinosteroid signaling pathways	serk2 for	TGGCAGACGGTTCGTTAGTC
				serk2 rev	CAGGTTCCGATGTACAGCCA
prd1	LOC111806591	Cp4.1LG12g04800	involved in meiotic recombination and in meiotic double strand break repair	prd1 for	GTGAGTGAAGCTGACGGTGA
				prd1 rev	AGCATATACACCTGACGCCG
mnd1	LOC111780437	Cp4.1LG18g03910	binds DNA and stimulates the recombinase activity of RAD51 in meiosis	mnd1 for	TGCGAAACGGCTTCACCCTT
				mnd1 rev	ATCTTCTCGCGCTTCTCTTC
pdr2	LOC111798428	Cp4.1LG07g09350	P-type ATPase cation pumps	prd2 for	GCACTTACAAGCGGAGAAGG
				prd2 rev	AACGGTTACTCGCTTGCTCA
msh2	LOC111780449	Cp4.1LG18g07460	DNA mismatch repair protein	msh2 for	GCCTCTAGCTGTCCAACTCC
				msh2 rev	CAGGGGTGCCTACTTCCTTC
xri	LOC111794632	-	required for post-meiotic stages of pollen development	xri for	AGGTTGGATTGCTGATTGCC
				xri rev	TGATTGTCCGAAGTCCCAGC
cyca2	LOC111808394	Cp4.1LG13g04500	core cell cycle gene involved in meiosis II	cyca2 for	AAGCACGTGGCGAAGAAGTA
				cyca2 rev	AGCCGCCATTGGAGTACAAA

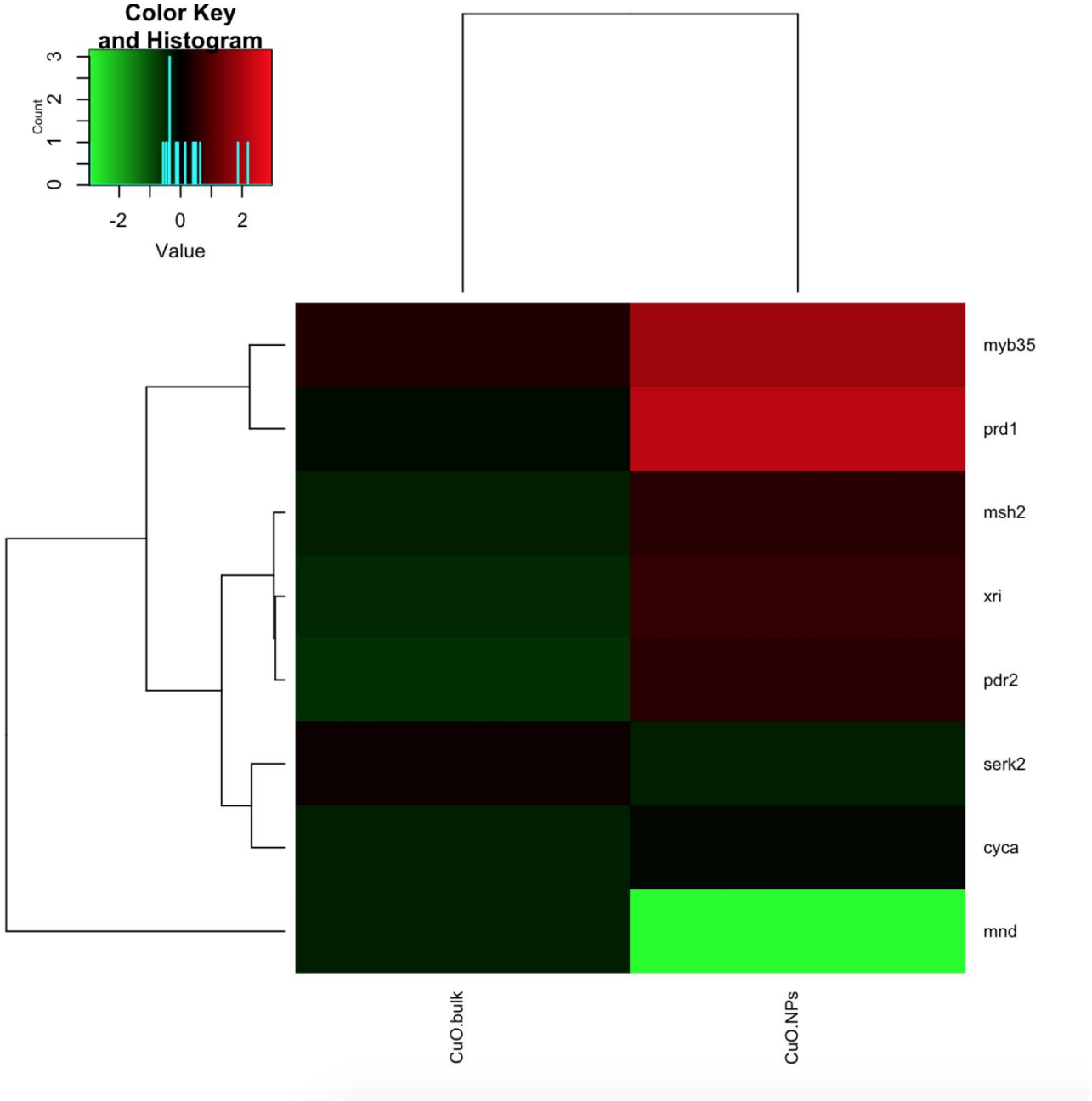

Figure S11. Heatmap representing quantitative real time PCR results on genes involved in meiosis and gametogenesis in *C. pepo*, using primers designed on genes identified in the yeast *Saccharomyces cerevisiae* (Table S5). Data showed a certain level of modulation of genes expecially in case of CuO NPs (mnd, prd1, myb35), while there are no significan changes in expression profile in case of CuO bulk.

Linear Combination Fitting (LCF) analysis of XANES spectra

Zucchini roots and flowers thin section samples were investigated by means of XRF mapping and XAS. Orienting on the basis of the elemental distribution in the XRF maps, XANES spectra at the Fe, Cu and Zn K-edges were acquired on selected areas (enriched in the chemical species of interest), as reported in Figure S12. In all the root and flowers samples, P, S, Cl, K, Ca, Fe, Ni, Cu and Zn fluorescence lines were detected, among which Ca is undoubtedly the most abundant. Some differences in the relative peak intensities were also identified depending on the treatment: For both series, samples treated with $CuSO_4$ have lower amounts of Cl, K and Fe but higher amount of S, Cu and Zn; CuO NPs treated samples have the highest amount of Cu whereas CuO bulk treated samples are the most similar to the untreated control. XANES data collected at Cu K-edge were modelled using Cu foil; CuO and Cu_2O reference compounds. Despite the low signal to noise ratio, the collected spectra appear to be quite similar. This is confirmed by LCF results, which largely highlight the presence of Cu^{2+}. XANES data collected at Zn K-edge were modelled using the following reference compounds: Zn foil; ZnO; $Zn(C_4H_6O_4)$ (Zn acetate anhydrous); $Zn_3(C_6H_5O_7)_2$ (Zn citrate); $Zn_3(PO_4)_2$ (Zn phosphate); $ZnSO_4*7H_2O$ (Zn sulphate heptahydrate); $ZnSO_4*H_2O$ (Zn sulphate monohydrate). All the spectra collected at the Zn K-edge are quite similar. Indeed, the obtained results show that in both root samples, all the Zn is in form of salts (oxidation state +2). Zn K-edge XANES spectra were collected also on the flower sample treated with bulk CuO, but the low signal to noise ratio prevented LCF analysis; however, considering the similarity of the edge position and the shape of the absorption edge with respect to that of root samples, the Zn chemical environment is probably the same. XANES data collected at Fe K-edge were modeled using the following reference compounds: Fe foil; αFe_2O_3 (hematite); $FeCr_2O4$ (chromite); $FeSO_4$ (Fe sulphate); Fe_3O_4 (magnetite); $FeNO_3$. The obtained results show that Fe chemical environment is different in the investigated samples. Indeed, the position of the absorption edge and pre-edge features indicate the presence of an important fraction of metallic Fe in sample Flower untreated control, besides a small amount of Fe^{2+} and Fe^{3+}.

Root CuO bulk sample seems to contain both Fe^{2+} and Fe^{3+} with also a fraction of Fe in tetrahedral coordination (justified by the higher intensity of the pre-edge peaks) whereas in sample Root CuO NPs, Fe^{3+} in octahedral coordination is dominant (lower pre-edge peaks intensity and higher white line). These results will need further investigations to elucidate the role of Fe.

a

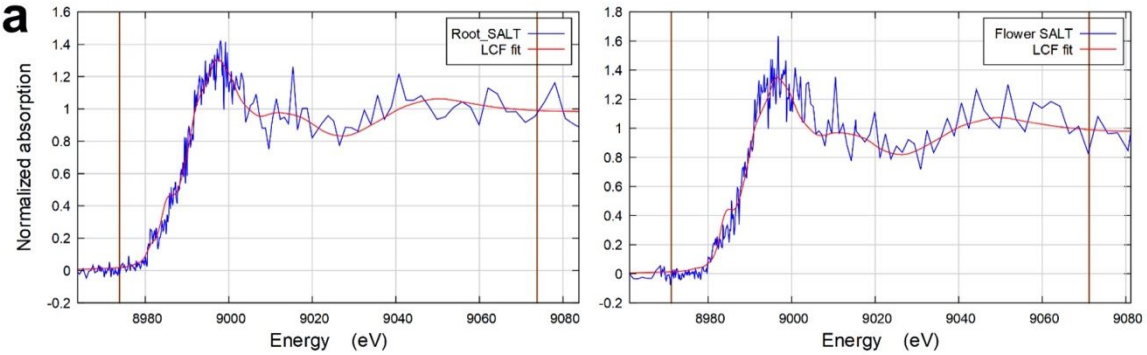

Sample	Metal Cu Cu^0	Cu_2O Cu^{1+}	CuO Cu^{2+}	Sum
Root_SALT	-	17 (4)	83 (6)	100
Flower_SALT	-	6 (4)	94 (6)	100

b

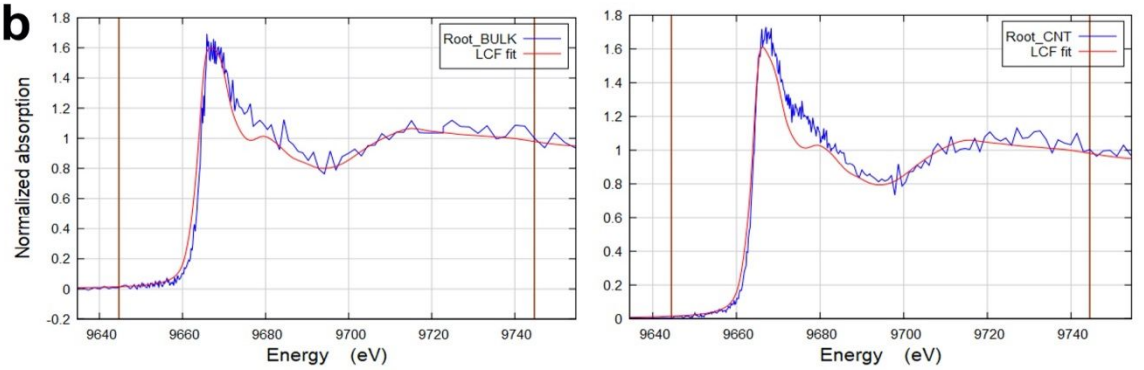

Sample	Metal Zn	ZnO	Zn sul. mono	Zn sul. hepta	Zn citrate	Zn acetate	Sum
Root_BULK	-	-	65 (23)	-	35 (11)	-	100
Root_CNT	-	-	-	52 (10)	22 (18)	24 (7)	100

c

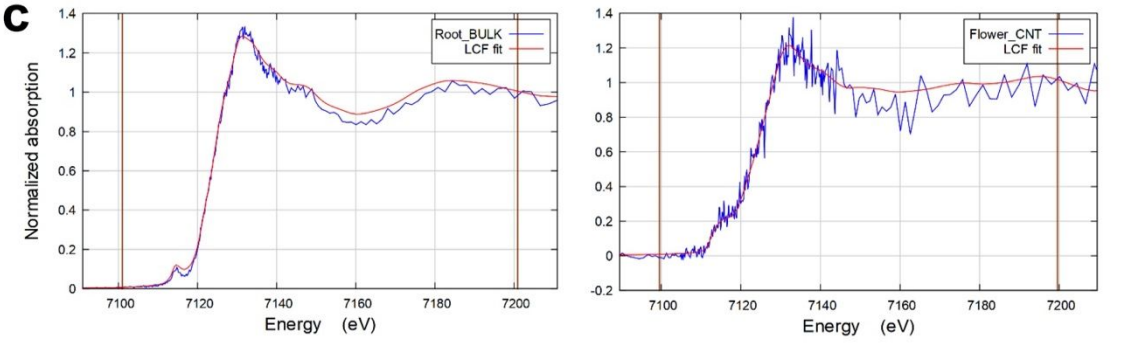

Sample	Metal Fe Fe^0	$FeCr_2O_4$ Fe^{2+} (VI)	$FeSO_4$ Fe^{2+} (VI)	Fe_3O_4 Fe^{2+} (VI) Fe^{3+} (IV+VI)	$FeNO_3$ Fe^{3+} (VI)	αFe_2O_3 Fe^{3+} (VI)	Sum
Root_BULK	-	-	5 (3)	71 (5)	-	24 (6)	100
Root_NP	-	4 (3)	-	19 (10)	-	77 (5)	100
Flower_CNT	54 (8)	9 (5)	7 (4)	-	30 (9)	-	100

Figure S12. XANES fit obtained through Linear Combination Fitting (LCF) analysis on the merged spectrum and relative K-edge data (reported quantities are percentage) collected at (a) Cu K-edge on samples Root_CuSO4 (left) and Flower_CuSO4 (right); (b) Zn K-edge on sample Root_CuO bulk (left) and Root_untreated control (right) and (c) Fe K-edge on samples Root_CuO bulk (left) and Flower_untreated control (right); roman numbers indicate the coordination geometry of the Fe atoms in the reference compounds used for the LCF.

Table S6. EXAFS multiparameter fit details for studied samples and reference compounds

Root_CuO				*Flower CuO*		
	R (Å)	N	σ^2 (Å^2)	R (Å)	N	σ^2 (Å^2)
Cu-O	1.94	4.00	0.003(9)	1.95	3.00	0.002(1)
Cu-O	2.73	1.00	0.001(3)	2.83	2.00	0.002(2)
Cu-Cu	2.98	3.00	0.023(7)	3.00	2.00	0.012(4)
Cu-Cu	3.49	2.00	0.023(7)			
Cu-O	3.68	2.00	0.001(3)	3.79	4.00	0.002(2)
Cu-Cu	3.82	3.00	0.023(7)	4.05	2.00	0.012(4)
Cu-O	4.34	4.00	0.001(3)	4.26	4.00	0.002(2)
Root CuO NPs				*Flower CuO NPs*		
Cu-O	1.94	3.00	0.0010(3)	1.95	3.00	0.0014(6)
Cu-O	2.67	1.00	0.002(1)	2.79	1.00	0.008(3)
Cu-Cu	2.92	3.00	0.017(2)	2.95	2.00	0.010(2)
Cu-Cu	3.55	2.00	0.017(2)			
Cu-O	3.69	2.00	0.002(1)	3.74	2.00	0.008(3)
Cu-Cu	3.82	3.00	0.017(2)	3.98	2.00	0.010(2)
Cu-O	4.36	5.00	0.002(1)	4.30	4.00	0.008(3)
Root $CuSO_4$				*Flower $CuSO_4$*		
Cu-O	1.94	4.00	0.005(1)	1.93	4.00	0.003(1)
Cu-O	2.65	1.00	0.008(3)	2.80	1.00	0.005(9)
Cu-Cu	2.90	5.00	0.024(4)	2.93	1.00	0.005(2)
Cu-Cu	3.52	4.00	0.024(4)	3.79	4.00	0.005(2)
Cu-O	3.71	4.00	0.008(3)			
Cu-Cu	3.71	4.00	0.024(4)	4.02	4.00	0.005(2)
Cu-O	4.28	5.00	0.008(3)	4.27	4.00	0.005(9)
CuO (bulk)				*CuO (NPs)*		

	1.95	4	0.0033(8)	1.95	4	0.0020(9)
$CuSO_4$						
	1.94	4	0.003(2)			

Notes: Accuracy on path length can be estimated as 0.01 Å for I shell paths and as 0.007*R for higher coordination shells. Only first shell paths are reported for model compounds. CuO bulk and CuO NPs were fitted to the tenorite structure up to R=5.8 Å with a final discrepancy between theoretical and fitted path distances of 0.01*R Å,^{2} using the correlated Debye model in order to compute Debye-Waller factors for each path and employing two different variables: one for the I shell (σ^2) and one for the higher coordination shells, which resulted equal to 367(15) and 342(14) K for bulk and NPs, respectively. For $CuSO_4$, due to the presence of two different Cu sites, only the first shell was fitted, resulting S_0^2 is 0.5. S_0^2 was fitted to 0.75 in CuO (bulk) and fixed to 0.7 in CuO (NPs) and plant samples. Fits were performed using a k range comprised between 3 and 11 Å^{-1}.

References

1. Liu, J.; Qu L-Q. Meiotic and Mitotic Cell Cycle Mutants Involved in Gametophyte Development in Arabidopsis. *Molecular Plant*. **2008**, 1(4), 564-574. Doi: 10.1093/mp/ssn033.
2. E. Sevillano, H. Meuth, J. J. Rehr. Extended x-ray absorption fine structure Debye-Waller factors. I. Monatomic crystals. *Phys. Rev. B*. **1979**, 20, 4908. Doi: 10.1103/PhysRevB.20.4908